Molecular Electronics

Deutsche Ausgabe: DOI: 10.1002/ange.201608131
Internationale Ausgabe: DOI: 10.1002/anie.201608131

A Unique Blend of 2-Fluorenyl-2-anthracene and 2-Anthryl-2-anthracence Showing White Emission and High Charge Mobility

Mengyun Chen, Yang Zhao, Lijia Yan, Shuai Yang, Yanan Zhu, Imran Murtaza, Gufeng He, Hong Meng,* and Wei Huang**

Abstract: *White-light-emitting materials with high mobility are necessary for organic white-light-emitting transistors, which can be used for self-driven OLED displays or OLED lighting. In this study, we combined two materials with similar structures—2-fluorenyl-2-anthracene (FlAnt) with blue emission and 2-anthryl-2-anthracence (2A) with greenish-yellow emission—to fabricate OLED devices, which showed unusual solid-state white-light emission with the CIE coordinates (0.33, 0.34) at 10 V. The similar crystal structures ensured that the OTFTs based on mixed FlAnt and 2A showed high mobility of 1.56 $cm^2 V^{-1} s^{-1}$. This simple method provides new insight into the design of high-performance white-emitting transistor materials and structures.*

Multifunctional organic semiconductor materials are of great interest for applications in organic electronics and relatively simple device-fabrication processes.[1] Organic light-emitting diodes (OLEDs) usually need to be driven by field-effect transistors, which entangle the device structure.[2] Organic light-emitting transistors (OLETs), which combine OLEDs and organic thin-film transistors (OTFTs), make self-driven organic light-emitting devices possible, thus simplifying the structure of OLED lighting and displays.[3] Perepichka and co-workers reported 2-(4-hexylphenylvinyl)anthracene (HPVAnt) as a blue-emitting material with a high mobility of 1.5 $cm^2 V^{-1} s^{-1}$ for OLETs.[4] White-emitting OLETs have great potential for their use in self-driven OLED lighting and displays, but to the best of our knowledge, so far there is no report on materials with white emission and simultaneous high mobility, although numerous studies have focused on materials with either white emission or high mobility.[5] It is known to be difficult to prepare small-molecule organic materials with single-component white emission, except in the cases of excimers or electromers. However, the combination of two high-mobility materials with different emission colors to achieve white emission while maintaining high mobility could potentially enable such multifunctionalization.

Anthracene is widely used in high-charge-transfer materials and also has superior light-emitting properties, whereas highly rigid fluorene is an excellent candidate for luminescence.[6] Initially, we envisioned that if we link a fluorene unit to an anthracene core, the resulting compound 2-fluorenyl-2-anthracene (FlAnt) could be a blue-emitting semiconductor. But much to our surprise, this compound showed broad photoluminescence (420–700 nm) covering the visible-light spectrum and emitted pure white light with the CIE coordinates (0.33, 0.34) at 10 V in single-emitting-component OLEDs.

Serendipitously, when we repeated the experiment, we found that the white emission was actually a combined effect of FlAnt, with deep-blue emission, and another material 2-anthryl-2-anthracence (2A), with greenish-yellow emission, which was introduced into FlAnt as a by-product. These two materials are hard to separate by sublimation, as they have similar thermal properties, in addition to a similar crystal packing structure. However, we managed to separate pure FlAnt and 2A by using the solubility difference of FlAnt and 2A in hot toluene. By comparing the photoluminescence spectra of thin films of each of the two materials and combinations of the materials with different ratios of pure FlAnt and 2A, we worked out that the ratio of FlAnt and 2A should be about 1:9 to serve our purpose. Herein, we report the optical and charge-transfer properties of pure FlAnt, pure 2A, and the 1:9 mixture (named Mixture1/9; see the mass spectra in Figure S1 and PL spectra in Figure S2a of the Supporting Information).

It is normal to achieve white emission in OLEDs by combining a greenish-yellow-emitting material and a blue-emitting material, but the mobility is seriously affected as a result of impurity.[7] However, in our system, to our surprise, the OTFTs based on mixed FlAnt and 2A showed high mobility up to 1.56 $cm^2 V^{-1} s^{-1}$, as a result of the similar crystal structures of these two materials. The realization of white emission with simultaneous high mobility, by the combination of two materials, should enable the development of self-driven OLED lighting and displays.

Compounds FlAnt and 2A were obtained by the Suzuki coupling of 2-bromoanthracene and a fluorenyl or anthra-

[*] M. Chen, Y. Zhao, L. Yan, Y. Zhu, I. Murtaza, Prof. Dr. H. Meng, Prof. Dr. W. Huang
Key Laboratory of Flexible Electronics (KLOFE) and Institute of Advanced Materials (IAM), Jiangsu National Synergetic Innovation Centre for Advanced Materials (SICAM), Nanjing Tech University
30 South Puzhu Road, Nanjing 211816 (China)
E-mail: iamhmeng@njtech.edu.cn
iamwhuang@njtech.edu.cn
S. Yang, Dr. G. He
National Engineering Laboratory for TFT-LCD Materials and Technologies
Department of Electronic Engineering, Shanghai JiaoTong University
Shanghai 200240 (China)
E-mail: gufenghe@sjtu.edu.cn
I. Murtaza
Department of Physics, International Islamic University
Islamabad 44000 (Pakistan)
Supporting information and the ORCID identification number(s) for the author(s) of this article can be found under http://dx.doi.org/10.1002/anie.201608131.

 © 2017 Wiley-VCH Verlag GmbH & Co. KGaA, Weinheim

cenyl boronic acid ester (Scheme 1), and their identity was confirmed by mass spectrometry and elemental analysis. Thermogravimetric analysis (TGA) showed a 5% weight loss at 342°C for FlAnt and 350°C for 2A (see Figure S2b), which reveals the high thermal stability of FlAnt and 2A. Differential thermal analysis (DSC) under N_2 showed a reversible process of melting and recrystallization with a melting point of 250°C for FlAnt and 324°C for 2A (see Figure S2c).

Optical characterization was carried out both in the thin-film phase (the materials were deposited on quartz) and in the solution phase. Both materials emitted blue light when dissolved in 1,2-dichlorobenzene, with a fluorescence lifetime of 5.05 ns for FlAnt and 1.47 ns for 2A at an emission wavelength of 430 nm (see Figure S3 for UV-Vis and photoluminescence (PL) spectra of FlAnt and 2A in 1,2-dichlorobenzene solution and Figure S4 for time-resolved fluorescence spectra in solution), and the photoluminescence quantum yields were about 58.8% for FlAnt and 28.0% for 2A in solution. We found that the radiative decay rates ($k_f = \Phi/\tau$) were 0.12 ns^{-1} for FlAnt and 0.19 ns^{-1} for 2A in solution.

The band gaps of FlAnt and 2A were calculated, from the onset wavelength in the UV-Vis spectrum in the thin film (Figure 1a), to be 2.85 eV for FlAnt and 2.76 eV for 2A. Thin films were deposited on a glassy carbon electrode and subjected to cyclic voltammetry (CV; see Fig-

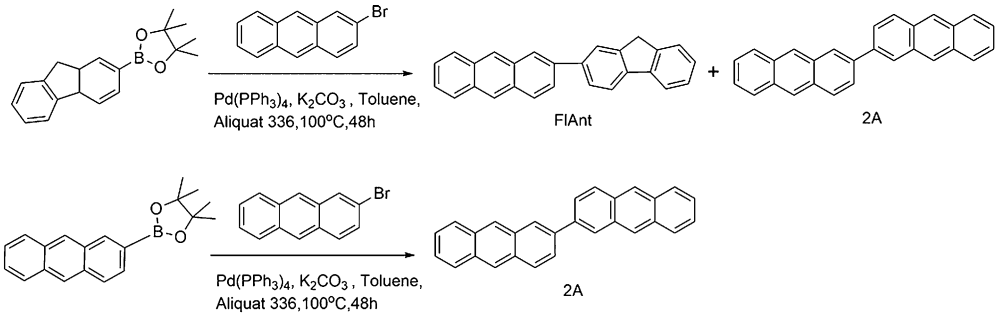

Scheme 1. Synthesis of FlAnt (with the side product 2A) and 2A.

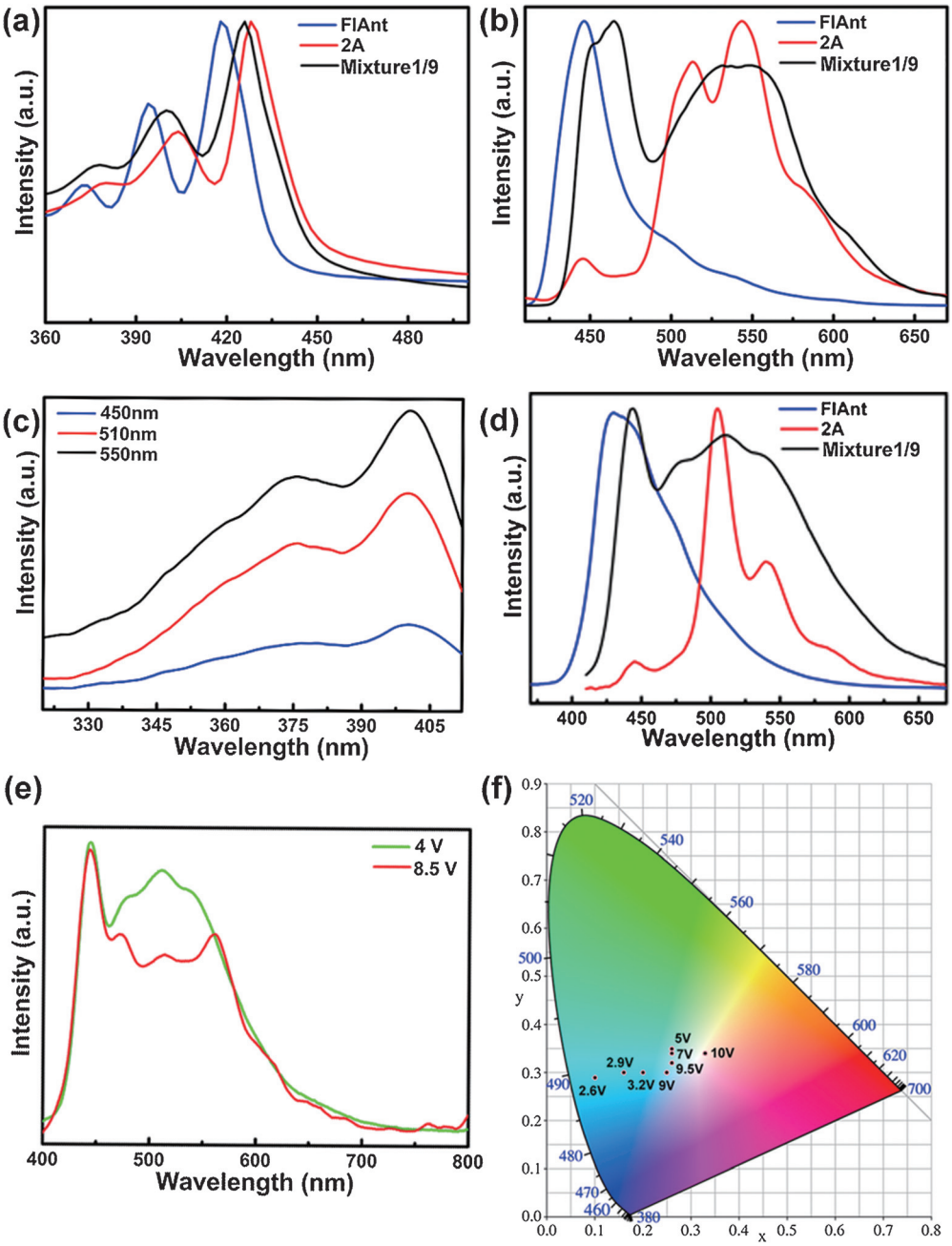

Figure 1. a) Optical absorption spectra; b) PL spectra in the thin films deposited on quartz; c) excitation spectra of 2A at different emissions in the thin film; d) EL spectra in OLEDs based on FlAnt, 2A, and Mixture1/9; e) EL spectra of Mixture1/9 at 4 and 8.5 V; f) CIE coordinates at different driving voltages in OLED devices based on Mixture1/9.

© 2017 Wiley-VCH Verlag GmbH & Co. KGaA, Weinheim

ure S2 d), which showed an oxidation potential of 0.90 V for FlAnt and 0.95 V for 2A. The calculated deep HOMO levels of −5.50 and −5.55 eV favor the high environmental stability of FlAnt and 2A, respectively. The thermal, optical, and electrochemical parameters of FlAnt and 2A are listed in Table S1 of the Supporting Information.

Figure 1 b shows the photoluminescence spectra of FlAnt and 2A in the solid state. To our surprise, FlAnt showed a deep-blue emission with CIE coordinates of (0.16, 0.11), whereas 2A demonstrated a broad yellow emission centered at 550 nm in addition to blue emission at 450 nm, which constitute a greenish-yellow emission with CIE coordinates of (0.30, 0.55). Figure 1 c shows the similar excitation spectra for emissions at 450, 510, and 550 nm in the thin film of 2A, which demonstrates the same source of these three emissions and thus excludes the formation of new fluorophore aggregates.[5a] The electroluminescence (EL) spectrum of 2A shown in Figure 1 d is similar to the PL spectrum in the thin film, which excludes the possibility of the formation of electromers and exciplexes in solid-state films.[5c] Thus, the yellow emission from 2A can be attributed to the excimers. Photoluminescence images of the powders are shown in Figure S5 of the Supporting Information.

To correlate the optoelectronic properties with the molecular-packing structure, we grew single crystals of FlAnt and 2A by sublimation for X-ray crystal-structure analysis.[8] The FlAnt molecule keeps a distance of 5.037–6.049 Å from the surrounding molecules, whereas the 2A molecule keeps a shorter distance of 4.676–5.958 Å (Figure 2). Thus, we assume that the two molecules with the shortest distance of 4.676 Å tend to form excimers: When one of the molecules becomes an exciton, it combines with the adjacent molecule to form an excimer for the sake of lowering the energy, which reduces the blue emission and gives narrow-band-gap light emission. The fluorescence quantum yield in the thin films of 2A is about 13.9 %, which is lower than that

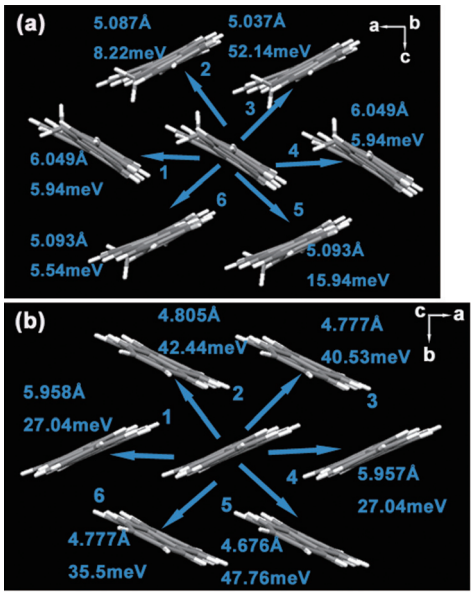

Figure 2. a) Molecular packing of a) the FlAnt single crystal and b) the 2A single crystal.

of FlAnt (about 15.7 %) as a result of a stronger intermolecular force at the excitation wavelength of 370 nm. It was found that the fluorescence lifetime for FlAnt at 450 nm was 1.93 ns (see Figure S4 for time-resolved fluorescence spectra of the thin films). The emissions from 2A at 450, 510, and 550 nm had unequal fluorescence lifetimes of 0.55, 5.33, and 7.34 ns, respectively, which further prove a difference in emission at 450 and 550 nm.

We fabricated OLEDs with the structure indium tin oxide (ITO)/MoO_3 (1 nm)/NPB (60 nm)/FlAnt (20 nm)/TPBi (40 nm)/LiF (1 nm)/Al (OLED-1; see Figure S6 a) to investigate the electroluminescence properties of FlAnt. *N*,*N*′-bis(naphthalen-1-yl)-*N*,*N*′-bis(phenyl)benzidine (NPB) and 1,3,5-tri(1-phenyl-1*H*-benzo[*d*]imidazol-2-yl)phenyl (TPBi) were chosen as the hole- and electron-transfer material, respectively. The electroluminescence spectra are shown in Figure 1 d. The OLEDs based on FlAnt showed deep-blue emission with CIE coordinates of (0.16, 0.11) and performed well with a low turn-on voltage of 2.7 V, a high brightness of 2778 cd m^{-2} at 10 V, and an external quantum efficiency (EQE) of 0.91 % (see Figure S7 a,d). Similarly, OLEDs based on 2A adopted the structure ITO/HAT-CN (30 nm)/HTL1 (50 nm)/HTL2 (10 nm)/2A (20 nm)/ETL1:Liq (30 nm)/Liq (1 nm)/Al (OLED-2; see Figure S6 b). Dipyrazino[2,3-*f*:2′,3′-*h*]quinoxaline-2,3,6,7,10,11-hexacarbonitrile (HAT-CN)was chosen as hole-injection material, *N*,*N*,11-tri([1,1′-biphenyl]-4-yl)-11*H*-benzo[*a*]carbazol-5-amine (HTL1) and 11-(4-([1,1′-biphenyl]-4-yl)quinazolin-2-yl)-8-(9-phenyl-9*H*-carbazol-3-yl)-11*H*-benzo[*a*]carbazole (HTL2) were chosen as the hole-transfer material, and 2-(4-(9,10-di(naphthalen-2-yl)anthracen-2-yl)phenyl)-1-phenyl-1*H*-benzo[*d*]imidazole:lithium 8-hydroxyquinolinolate (ETL1:Liq) was chosen as the electron-transfer material. The OLEDs based on 2A emitted greenish-yellow light with the CIE coordinates (0.29, 0.49) and operated with a low turn-on voltage of 2 V, a high brightness of 5655 cd m^{-2} at 10 V, and an EQE of 0.46 % (see Figure S7 b,e).

The PL of the thermally deposited thin films of Mixture1/9 showed much broader emission and CIE coordinates of (0.28, 0.36). The OLED devices based on this simple mixture with the OLED-1 device structure showed a low turn-on voltage of 3 V, a high brightness of 2560 cd m^{-2} at 10 V, EQE of 0.16 % and exhibited white emission with a combination of blue and broad greenish-yellow emissions (see Figure S7 c,f). When the driving voltage increased from 4 to 8.5 V, the green part of the emission (515 nm) decreased considerably, and the red part of the emission (610 nm) increased (Figure 1 e), so that the CIE_x coordinate increased from 0.25 to 0.26, and the CIE_y coordinate decreased sharply from 0.35 to 0.31, towards white emission. The CIE coordinates moved from (0.1, 0.29), corresponding to bluish-green emission, to (0.33, 0.34), corresponding to pure-white emission, when the driving voltage was increased from 2.6 to 10 V (Figure 1 f). The simple mixing of FlAnt and 2A and evaporation in a source stove provides a new and straightforward method for the production of white-emitting OLEDs.

The X-ray crystallographic results (Figure 2) showed that the FlAnt crystal belongs to the *P*2(1)/*c* space group with a monoclinic crystal structure and crystal parameters of *a* =

© 2017 Wiley-VCH Verlag GmbH & Co. KGaA, Weinheim

6.0492(4), $b = 37.386(2)$, $c = 15.646(1)$ Å, $\beta = 90.311(3)°$, whereas the 2A crystal belongs to the $P1n1$ space group with a monoclinic crystal structure and crystal parameters of $a = 5.9575(10)$, $b = 7.4678(12)$, $c = 38.764(7)$ Å, $\beta = 90.067(9)°$. The FlAnt and 2A molecules both adopt typical herringbone packing structures, with herringbone angles of 52.93 and 51.34°, respectively.

To evaluate the charge-transfer properties of the material, we calculated the mobilities of FlAnt and 2A with the Amsterdam Density Functional (ADF) software, using PW91 functional and triple-zeta 2 plus polarization basis set (GGA:PW91/TZ2P), and Gaussian 09 D01 version software, using B3LYP(D3) functional and 6-311G(d, p)[2] basis set, for modeling based on single-crystal structures. The coplanarity in the 2A molecule, with a torsion angle of 0.2°, is much better than that of FlAnt with a torsion angle of 7.06°, thus ensuring stronger π–π stacking. The coplanarity and thus the closer distances between the molecules of 2A ensure a larger transfer integral for the 2A molecules than for the FlAnt molecules. When one 2A molecule was chosen as the center, the transfer integrals for the surrounding six groups were between 27.04 and 47.76 meV, but for the FlAnt molecules, the transfer integrals for six groups were small and quite inhomogeneous at different orientations. Only the transfer integral of 52.14 meV between molecule 3 and the central molecule, which is almost 10 times larger than for the other groups, is comparable with those found for 2A (Figure 2b).[9] Furthermore, the reorganization energy of 2A (97.9 meV) is much smaller than that of FlAnt (185 meV), so that the calculated mobility of 2A (0.52 $cm^2 V^{-1} s^{-1}$) is about twice that of FlAnt (0.25 $cm^2 V^{-1} s^{-1}$).

We fabricated OTFTs (see Figure S6c for the structure) to evaluate the charge-transport properties of FlAnt and 2A. FlAnt-based OTFTs provided a highest mobility of up to 0.22 $cm^2 V^{-1} s^{-1}$ with an I_{on}/I_{off} ratio of about 2.36×10^5, while 2A-based OTFTs showed the highest mobility of 3.19 $cm^2 V^{-1} s^{-1}$ and an I_{on}/I_{off} of about 2.13×10^6. Mixture1/9 in OLED devices showed white emission, so we also studied the influence of the mixture on mobility, and fabricated OTFTs with Mixture1/9, which showed high mobility of up to 1.56 $cm^2 V^{-1} s^{-1}$ and an I_{on}/I_{off} ratio of about 2.29×10^6, thus demonstrating that white emission was realized with no serious loss of mobility (Figure 3). Owing to the similarity of the crystal structures of FlAnt and 2A, the doping of FlAnt does not form influential charge-transfer traps.

For the purpose of studying the crystallinity and surface morphology of the thin films, thin-film X-ray diffraction (XRD) and atomic force microscopy (AFM) were conducted on films deposited on the *n*-octadecyltrichlorosilane (OTS)-treated SiO_2/Si. Several strong peaks were observed in the XRD patterns (see Figure S8), thus indicating the high crystallinity of the thin films of FlAnt and, in particular, 2A.[10] The four peaks at $2\theta = 4.89$, 9.68, 14.50, and 19.22° for FlAnt and $2\theta = 4.59$, 9.27, 13.79, and 18.49° for 2A in the thin-film XRD patterns indicate the planes (0, 2, 0), (0, 4, 0), (0, 6, 0), and (0, 8, 0) of the FlAnt crystal and (0, 0, 2), (0, 0, 4), (0, 0, 6), and (0, 0, 8) of the 2A crystal, thus showing that the molecules are grown perpendicular to the substrate with π–π stacking parallel to the substrate, which is favorable for carrier transport. The thin film deposited with Mixture1/9 showed peaks at $2\theta = 4.73$, 9.34, 14.02, and 18.61°, which are higher values than those of pure 2A, thus indicating that doping with FlAnt changed the crystal lattice of 2A to some degree.[11]

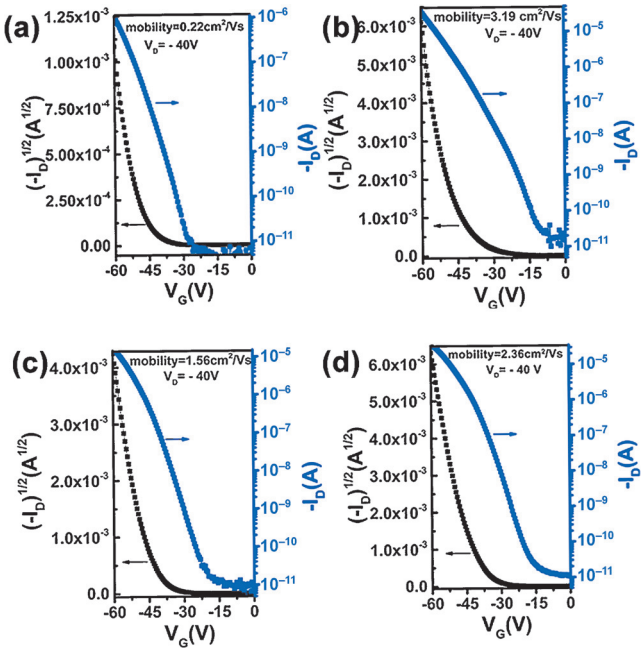

Figure 3. Transfer curves of the a) FlAnt-, b) 2A-, and c) Mixture1/9-based OTFTs at $T_{sub} = 25$ °C and d) Mixture1/9-based OTFT at $T_{sub} = 60$ °C.

The XRD observations are consistent with the terraced structures observed by AFM (Figure 4), which showed that the FlAnt and 2A molecules are grown layer-by-layer with step heights of approximately 1.869 nm for FlAnt (see Figure S9a and b), nearly equal to the length of the FlAnt molecule (1.759 nm), and of approximately 2.06 nm (see Figure S9c and d) for 2A, with a molecular length of 1.821 nm. In the thin film of Mixture1/9, the terraced

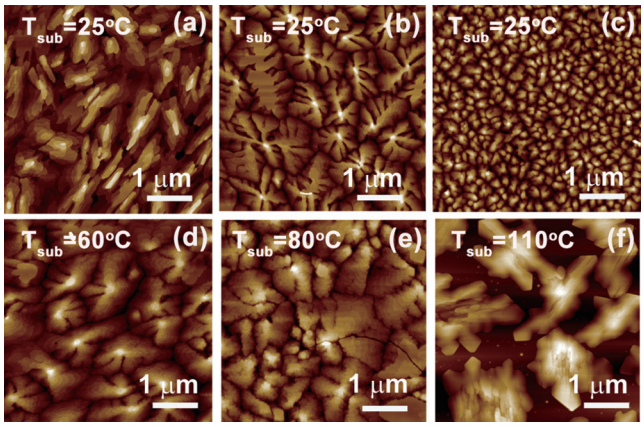

Figure 4. a,b) AFM images of thin films of FlAnt and 2A deposited on OTS-treated SiO_2/Si at $T_{sub} = 25$ °C; c–f) AFM images of thin films of Mixture1/9 deposited on OTS-treated SiO_2/Si at different substrate temperatures: c) $T_{sub} = 25$ °C, d) $T_{sub} = 60$ °C, e) $T_{sub} = 80$ °C, f) $T_{sub} = 110$ °C.

 © 2017 Wiley-VCH Verlag GmbH & Co. KGaA, Weinheim

structure was still present, with similar steps of about 1.750 nm (see Figure S9e and f). According to the AFM images, FlAnt grows into elliptical grains, which is consistent with the shape of the rod-like structure of the single crystal (see Figure S5b) and can be explained by the stronger intermolecular effect between molecule 3 and the central molecule than with other groups. This kind of inhomogeneous transfer integral leads to the limitation of hole-transfer to one direction and thus a serious decrease in mobility. However, the 2A molecules grow into uniform grains with considerable transfer integrals for all orientations shown in Figure 2b. In the case of the mixture, a trace amount of FlAnt influences the growth of 2A, and the grains are much smaller than those of pure 2A but still follow the homogenous intermolecular force at different orientations. Thus, the homogeneous intermolecular force offers uniform charge-transfer possibilities for all orientations and is advantageous for increasing charge mobility among molecules.

The substrate temperature has proved to play a great role in molecular packing and thus OTFT performance.[12] Therefore, we fabricated OTFT devices based on Mixture1/9 with substrate temperatures ranging from room temperature to 110 °C (see Figure S10 for transfer and output curves and Table 1 for performance parameters). The AFM images in Figure 4c–f show the thin-film morphology at different substrate temperatures and thus explain the change in mobility. When T_{sub} increased from 25 to 60 °C, the mobility increased from $(1.09 \pm 0.30)\ cm^2 V^{-1} s^{-1}$ to $(1.94 \pm 0.34)\ cm^2 V^{-1} s^{-1}$ owing to the larger grains. Some cracks were also formed as a result of the increase in the substrate temperature.[13] Therefore, the mobility decreased to $(0.82 \pm 0.06)\ cm^2 V^{-1} s^{-1}$ at $T_{sub} = 80$ °C and $(0.12 \pm 0.02)\ cm^2 V^{-1} s^{-1}$ at $T_{sub} = 110$ °C. The roughness of the film deposited at $T_{sub} = 110$ °C was more than 4 times larger than that of the film deposited at $T_{sub} = 25$ °C. The substrate temperature thus has a great influence on the charge-transport properties of OTFTs.

In this study, we synthesized and studied the properties of the materials 2-fluorenyl-2-anthracene (FlAnt) and 2-anthryl-2-anthracence (2A). FlAnt emitted deep-blue light, whereas 2A emitted greenish-yellow light because of the formation of excimers as a result of close molecular distances in the thin film. OLED devices based on Mixture1/9 (FlAnt/2A 1:9) showed broad white emission when the voltage was higher than 7 V, thus leading to a pure white emission with CIE coordinates of (0.33, 0.34) at 10 V. As a result of the inhomogeneous intermolecular force at different orientations, charge transfer in FlAnt was limited along some orientations, so the mobility of FlAnt ($0.22\ cm^2 V^{-1} s^{-1}$) was much lower than that of 2A ($3.19\ cm^2 V^{-1} s^{-1}$; Table 1). To our surprise, the small amount of FlAnt doped in 2A to create Mixture1/9 did not seriously decrease the mobility of the material as compared to that of pure 2A. This behavior can be explained by the similar crystal structures of FlAnt and 2A.

Table 1: Performance of the FlAnt/2A-based OTFT devices.

Material	T_{sub} [°C]	μ_{max} [$cm^2 V^{-1} s^{-1}$]	μ [$cm^2 V^{-1} s^{-1}$]	I_{on}/I_{off}
FlAnt	25	0.22	0.14 ± 0.06	2.36×10^5
2A	25	3.19	2.98 ± 0.16	2.13×10^6
Mixture1/9	25	1.56	1.09 ± 0.30	2.29×10^6
Mixture1/9	60	2.36	1.94 ± 0.34	3.47×10^6
Mixture1/9	80	0.92	0.82 ± 0.06	4.45×10^5
Mixture1/9	110	0.14	0.12 ± 0.02	7.11×10^4

To the best of our knowledge, the combination of two materials has not been investigated previously with the aim of creating a new material showing white emission and simultaneous high mobility. On the basis of these findings, we now plan to develop a series of materials exhibiting white emission as well as high mobility for self-driven OLED displays or lighting.

Acknowledgements

This research was supported by the NSFC (51373075, 61136003), the National Research Foundation for the Doctoral Program (20133221110004), the National Basic Research Program of China (973 Program; No. 2015CB856505, 2015CB932200), the Natural Science Foundation of Jiangsu Province (BM2012010), Synergetic Innovation Center for Organic Electronics and Information Displays, Shenzhen Key Laboratory of Shenzhen Science and Technology Plan (ZDSYS20140509094114164), the Provincial Science and Technology Project of Guangdong Province (2015B090914002, 2014B090914003), and Guangdong Talents Project, Guangdong Academician Workstation (2013B090400016), and the Shenzhen Peacock Program (KQTD2014062714543296).

Keywords: molecular electronics · organic light-emitting diodes · organic optoelectronics · organic thin-film transistors · semiconductors

How to cite: *Angew. Chem. Int. Ed.* **2017**, *56*, 722–727
Angew. Chem. **2017**, *129*, 740–745

[1] O. Ostroverkhova, *Chem. Rev.* **2016**, *116*, 13279–13412.
[2] a) Q. Xu, H. M. Duong, F. Wudl, Y. Yang, *Appl. Phys. Lett.* **2004**, *85*, 3357; b) S. Zhang, W. X. Zhang, Z. Xi, *Chem. Eur. J.* **2010**, *16*, 8419–8426; c) J. Xiao, Y. Divayana, Q. Zhang, H. M. Doung, H. Zhang, F. Boey, X. W. Sun, F. Wudl, *J. Mater. Chem.* **2010**, *20*, 8167; d) J. Xiao, S. Liu, Y. Liu, L. Ji, X. Liu, H. Zhang, X. Sun, Q. Zhang, *Chem. Asian J.* **2012**, *7*, 561–564; e) J. Li, Y. Zhao, J. Lu, G. Li, J. Zhang, Y. Zhao, X. Sun, Q. Zhang, *J. Org. Chem.* **2015**, *80*, 109–113; f) G. Li, Y. Zhao, J. Li, J. Cao, J. Zhu, X. W. Sun, Q. Zhang, *J. Org. Chem.* **2015**, *80*, 196–203.
[3] a) A. Hepp, H. Heil, W. Weise, M. Ahles, R. Schmechel, H. V. Seggern, *Phys. Rev. Lett.* **2003**, *91*, 157406; b) R. Capelli, S. Toffanin, G. Generali, H. Usta, A. Facchetti, M. Muccini, *Nat. Mater.* **2010**, *9*, 496–503.
[4] A. Dadvand, A. G. Moiseev, K. Sawabe, W. H. Sun, B. Djukic, I. Chung, T. Takenobu, F. Rosei, D. F. Perepichka, *Angew. Chem. Int. Ed.* **2012**, *51*, 3837–3841; *Angew. Chem.* **2012**, *124*, 3903–3907.
[5] a) Y. Liu, M. Nishiura, Y. Wang, Z. Hou, *J. Am. Chem. Soc.* **2006**, *128*, 5592–5593; b) J. Kalinowski, M. Cocchi, D. Virgili, V. Fattori, J. A. G. Williams, *Adv. Mater.* **2007**, *19*, 4000–4005; c) J. Li, D. Liu, C. Ma, O. Lengyel, C. Lee, C. Tung, S. Lee, *Adv. Mater.* **2004**, *16*, 1538–1544; d) T. Fleetham, J. Ecton, Z. Wang, N. Bakken, J. Li, *Adv. Mater.* **2013**, *25*, 2573–2576; e) Y. Yuan, G.

 © 2017 Wiley-VCH Verlag GmbH & Co. KGaA, Weinheim

Giri, A. L. Ayzner, A. P. Zoombelt, S. C. Mannsfeld, J. Chen, D. Nordlund, M. F. Toney, J. Huang, Z. Bao, *Nat. Commun.* **2014**, *5*, 3005; f) Y. Gao, X. Zhang, H. Tian, J. Zhang, D. Yan, Y. Geng, F. Wang, *Adv. Mater.* **2015**, *27*, 6753 – 6759.

[6] a) J. Liu, H. Zhang, H. Dong, L. Meng, L. Jiang, L. Jiang, Y. Wang, J. Yu, Y. Sun, W. Hu, A. J. Heeger, *Nat. Commun.* **2015**, *6*, 10032; b) J. Liu, H. Dong, Z. Wang, D. Ji, C. Cheng, H. Geng, H. Zhang, Y. Zhen, L. Jiang, H. Fu, Z. Bo, W. Chen, Z. Shuai, W. Hu, *Chem. Commun.* **2015**, *51*, 11777 – 11779; c) I. Cho, S. H. Kim, J. H. Kim, S. Park, S. Y. Park, *J. Mater. Chem.* **2012**, *22*, 123 – 129; d) S. Tao, Z. Peng, X. Zhang, P. Wang, C. S. Lee, S. T. Lee, *Adv. Funct. Mater.* **2005**, *15*, 1716 – 1721; e) S. M. King, I. I. Perepichka, I. F. Perepichka, F. B. Dias, M. R. Bryce, A. P. Monkman, *Adv. Funct. Mater.* **2009**, *19*, 586 – 591.

[7] a) B. W. D′Andrade, R. J. Holmes, S. R. Forrest, *Adv. Mater.* **2004**, *16*, 624 – 628; b) Y. Sun, S. R. Forrest, *Appl. Phys. Lett.* **2007**, *91*, 263503.

[8] CCDC 1499040 and 1508821 contain the supplementary crystallographic data for this paper. These data can be obtained free of charge from The Cambridge Crystallographic Data Centre.

[9] D. Zhang, L. Zhao, Y. Zhu, A. Li, C. He, H. Yu, Y. He, C. Yan, O. Goto, H. Meng, *ACS Appl. Mater. Interfaces* **2016**, *8*, 18277 – 18283.

[10] Y. Lei, P. Deng, M. Lin, X. Zheng, F. Zhu, B. S. Ong, *Adv. Mater.* **2016**, *28*, 6687 – 6694.

[11] L. Yan, Y. Zhao, H. Yu, Z. Hu, Y. He, A. Li, O. Goto, C. Yan, T. Chen, R. Chen, Y.-L. Loo, D. F. Perepichka, H. Meng, W. Huang, *J. Mater. Chem. C* **2016**, *4*, 3517 – 3522.

[12] J. H. Kim, J. Lee, S. Im, *J. Appl. Phys.* **2004**, *95*, 3733 – 3736.

[13] H. Meng, F. Sun, M. B. Goldfinger, G. D. Jaycox, Z. Li, W. J. Marshall, G. S. Blackman, *J. Am. Chem. Soc.* **2005**, *127*, 2406 – 2407.

Manuscript received: August 19, 2016
Final Article published: December 9, 2016

 © 2017 Wiley-VCH Verlag GmbH & Co. KGaA, Weinheim